

GENETICALLY-MODIFIED MACROPHAGES ACCELERATE MYELIN REPAIR

Vanja Tepavčević^{1,2,*}, Gaëlle Dufayet-Chaffaud¹, Marie-Stephane Aigrot¹, Beatrix Gillet-

Legrand¹, Satoru Tada¹, Leire Izaguirre², Nathalie Cartier^{1,*†}, and Catherine Lubetzki^{1,3,*†}

1

ONE SENTENCE SUMMARY: Targeted delivery of Semaphorin 3F by genetically-modified macrophages accelerates OPC recruitment and improves myelin regeneration

ABSTRACT

Despite extensive progress in immunotherapies that reduce inflammation and relapse rate in patients with multiple sclerosis (MS), preventing disability progression associated with cumulative neuronal/axonal loss remains an unmet therapeutic need. Complementary approaches have established that remyelination prevents degeneration of demyelinated axons. While several pro-remyelinating molecules are undergoing preclinical/early clinical testing, targeting these to disseminated MS plaques is a challenge. In this context, we hypothesized that monocyte (blood) -derived macrophages may be used to efficiently deliver repair-promoting molecules to demyelinating lesions. Here, we used transplantation of genetically-modified hematopoietic stem cells (HSCs) to obtain circulating monocytes that

¹ 1. INSERM UMR1127 Sorbonne Université, Paris Brain Institute (ICM), Paris, France.

2. Achucarro Basque Center for Neuroscience/University of the Basque Country, Leioa, Spain

3. AP-HP, Hôpital Pitié-Salpêtrière, Paris, France

* corresponding authors

† senior co-authors

overexpress Semaphorin 3F, a pro-remyelinating molecule. We show that Semaphorin 3F-expressing macrophages quickly infiltrate demyelinating spinal cord lesions, which increases oligodendrocyte progenitor cell recruitment and accelerates myelin repair. Our results provide a proof-of-concept that monocyte-derived macrophages could be used to deliver pro-remyelinating agents “at the right time and place”, suggesting novel means for remyelinating therapies in patients with MS.

INTRODUCTION

Preventing/reducing the progression of neurological disability in patients with multiple sclerosis (MS) is a major challenge. MS most frequently starts as a relapsing-remitting disease (RRMS), with episodes of neurological symptoms alternating with those of recovery. RRMS eventually evolves into secondary progressive MS (SPMS), characterized by development of permanent neurological handicap. A subset of patients directly enters the progressive phase (primary progressive MS (PPMS))¹.

Currently used treatments for MS are mostly immunomodulators and immunosuppressants. These reduce inflammatory bouts and related relapses in RRMS, but are largely ineffective in progressive disease¹ where accumulation of disability is the consequence of neuronal and axonal loss, partly independent of inflammation, and likely triggered by increased vulnerability of demyelinated axons². Remyelination (myelin regeneration) of demyelinated axons protects these from degeneration, as suggested by neuropathological studies of MS tissue², experiments using a model of demyelination³, and a longitudinal follow up of MS patients using myelin PET imaging⁴. Hence, development of remyelination-promoting strategies to prevent/reduce the accumulation of irreversible disability in patients with MS is a major therapeutic goal actively pursued worldwide⁵.

Remyelination failure in a subset of MS lesions is associated with depletion/low numbers of oligodendroglial cells⁶⁻⁹. Thus, stimulating oligodendrocyte progenitor cell (OPC) repopulation/recruitment to demyelinated areas may be crucial to enhance myelin repair. We and others have shown that local overexpression of the guidance molecule Semaphorin 3F (Sema3F) in a focal mouse model of demyelination increases OPC recruitment and accelerates remyelination^{8, 10}. As human OPCs express Sema3F receptors¹¹, a similar strategy may be beneficial for patients with MS. However, demyelinating MS lesions are disseminated in the CNS, which hampers the development of therapies that aim to stimulate local myelin repair.

Since MS lesions are associated with the presence of activated microglia and monocyte (blood)-derived macrophages¹, we hypothesized that myeloid lineage cells could be used as vehicles for targeted delivery of repair-promoting molecules. Here we focused on genetic modification of blood-derived cells rather than microglia as this approach is therapeutically more feasible. Thus, we transplanted genetically-modified hematopoietic stem/progenitor cells (HSCs) as means of obtaining circulating monocytes that overexpress Sema3F in mice. We show that Sema3F-carrying macrophages infiltrate demyelinating spinal cord lesions, which increases OPC recruitment and accelerates the onset of remyelination.

Our results provide a proof-of-concept that genetically-modified monocytes/macrophages can be used to enhance CNS remyelination, which may provide novel cues for implementing therapies to prevent/diminish neurological disability in patients with MS.

RESULTS

Donor-derived macrophages infiltrate demyelinating lesions

To investigate whether transplanted hematopoietic cell progeny targets demyelinating CNS lesions, we injected pre-conditioned mice intravenously with whole bone marrow (WBM) isolated from actin-GFP mice (Fig. 1A). At two months post-transplant, 72.6 ± 5.84 % of blood cells were GFP+. Moreover, 87.07 ± 9.7 % of blood CD11b+ cells (monocytes) were GFP+. Thus, monocytes in chimeric mice derive mostly from transplanted cells. (Fig. 1B)

We next induced demyelination in the spinal cord of chimeric mice by injecting lysolecithin (LPC). (Fig 1C)

LPC lesion is a widely used model of focal demyelination characterized by a temporally-defined sequence of events: 1) Demyelination-complete at 2-3 days post lesion (dpl); 2) myelin debris clearance by microglia/macrophages; 3) OPC repopulation (recruitment/proliferation)- 7 dpl; 4) OPC differentiation-maximal at 14 dpl; and 5) remyelination: onset-14 dpl, highly advanced- 21 dpl. We investigated the identity of graft-derived cells infiltrating LPC lesions, and the extent and chronology of their recruitment. At both 3 and 7 dpl, GFP+ cells were found in demyelinated areas. Co-labelling for GFP and CD11b/CD68, revealed that 91.5 ± 1.6 % of GFP+ cells were macrophages. Moreover, 47.5 ± 4.66 % of macrophages in the lesion were GFP+. Only occasional GFP+ cells were observed in spinal cord areas distant to the lesion. In the brain, some GFP+ cells were observed mostly in the areas containing perivascular/meningeal macrophages¹².

Therefore, graft-derived macrophages reliably target CNS lesions early after demyelination and hence represent appropriate molecular vehicles for stimulating OPC repopulation/myelin repair. Moreover, given that the median of 96.35% of circulating blood monocytes in these experiments were GFP+, we can assume that within demyelinated lesions, all blood-derived cells are GFP+, while resident CNS microglia/macrophages are GFP-. Thus, our results demonstrate early recruitment of both resident (GFP-) and blood-derived (GFP+) macrophages in LPC lesions.

Genetically modified HSCs secrete Sema3F that increases OPC migration in vitro

Next, we generated lentiviral vectors to overexpress Sema3F, a molecule that stimulates OPC recruitment and myelin repair^{8, 10}. We used a bicistronic lentiviral construction in which self-cleaving T2A sequence was inserted between the Sema3F- and GFP-encoding sequences, all under the control of PGK promoter (PGK-GFP-T2A-SemaF; Fig. S1). Thus Sema3F and GFP should be produced as separate proteins.

To verify the functionality of lentiviral-vector encoded Sema3F, we evaluated migration of adult OPCs in response to the supernatant from either non-transduced (NT)-, PGK-GFP-transduced-, or PGK-GFP-T2A-Sema3F-transduced HEK cells using transwell-chamber assay (Fig.2A). While number of migrated cells was similar between NT and PGK-GFP, it was 1.8-fold higher in Sema3F-GFP versus GFP (Fig. 2B). Next, we genetically modified HSCs in vitro to overexpress Sema3F. HSCs were isolated using magnetic-activated cell sorting (MACS) and transduced in vitro with PGK-GFP-T2A-Sema3F lentiviral vector or PGK-GFP vector (control). Transduced preparations were then expanded for 5 days (Fig. 2C). 35.78±5.27% of PGK-GFP-T2A-Sema3F- and 76.7±4.78% of PGK-GFP-transduced cells were GFP+ (Fig. 2D). This difference in transduction efficiency can be explained by a 30% greater size of the Sema3F-GFP transgene (Fig. S1).

Using western blot, we detected GFP expression in the lysate of both control and Sema3F-transduced cells, even though to a lesser extent in the latter (Fig. 2E), consistent with lower transduction efficiency of PGK-GFP-T2A-Sema3F vector. Sema3F was detected exclusively in the supernatant of PGK-GFP-T2A-Sema3F-transduced cells (Fig. 2E).

No differences in cell viability (propidium iodide and Viability 405/520 Fixable Dye labeled cells) or in the pattern of colony formation (proliferation/differentiation potential) were observed between GFP- and Sema3F-transduced HSC preparations (Fig. S2).

Therefore, transduction of HSC with PGK-GFP-T2A-Sema3F does not affect HSC viability and differentiation in vitro, but leads to secretion of Sema3F that, consistent with previous studies^{8,10}, increases adult OPC migration in vitro.

Hematopoietic reconstitution by transduced HSCs

Next, we transplanted female GFP and Sema3F-transduced HSCs (mixture of transduced and non-transduced cells) to preconditioned male recipient mice (GFP and Sema3F mice; Fig.2F). At 2 months post-grafting, qPCR for sex-containing region of the Y chromosome showed extensive reconstitution by transplanted (female) cells in both groups ($87.96 \pm 4.05\%$ GFP and $88.68 \pm 2.41\%$ Sema3F) (Fig. 2G). Flow cytometry analyses of GFP expression, used to investigate blood chimerism by transduced cells, revealed $76.7 \pm 4.78\%$ of GFP+ cells in GFP and $35.78 \pm 5.27\%$ in Sema3F group (Fig. 2H), consistent with lower transduction efficiency of PGK-GFP-T2A-Sema3F vector mentioned above.

We then investigated, by flow cytometry, differentiation of transduced (GFP+) cells into monocytes (CD11b+), B cells (CD19+), and T cells (CD3+). Interestingly, the percentage of GFP cells co-expressing CD11b was higher in Sema3F mice, while that of GFP+ cells co-expressing CD19 was lower. No difference in CD3+GFP+ cells was observed (Fig. 2I). However, the increase in CD11b+ over CD19+ cell generation by GFP+ cells did not affect the overall blood cell composition in chimeric mice as the percentages of total CD11b+, CD19+, and CD3+ cells in the blood were similar between the GFP and Sema3F mice (Fig. 2J). Therefore, Sema3F mice show normal blood composition.

Sema3F-carrying macrophages in demyelinating lesions

We next investigated the response of transgene-carrying cells to LPC-induced spinal cord demyelination. GFP+ cells were detected at 7 and 10 dpl in GFP and Sema3F mice with less cells in the latter (Fig. 3A-B, D-E, G). We investigated the correlation between the percentage of GFP+ cells in the blood and numbers of GFP+ cells in lesions using Prism and detected a strong correlation at both 7 ($R=0.81$) and 10 dpl ($R=0.66$). This indicates that numbers of GFP+ cells attracted to the lesions is primarily determined by GFP blood chimerism, which itself depends on transduction efficiency (lower for PGK-GFP-T2A-Sema3F). Therefore, Sema3F expression does not alter monocyte homing to demyelinating CNS lesions.

We analyzed whether recruited cells persist in the lesions once myelin repair is complete. At 60 dpl, numbers of GFP+ cells were decreased compared to earlier time points, and were similar between the two groups (Fig 3C,F-G). However, as we could only analyze 2 GFP and 3 Sema3F chimeras, we cannot deduce whether Sema3F-expressing cells are differentially retained in the CNS.

Interestingly, while basically all GFP+ cells at 7 and 10 dpl had morphology of myelin-phagocytosing macrophages (large, round), we also observed ramified GFP+ cells in the lesion-neighbouring tissue at all time points and within the lesion itself at 60 dpl (Fig. S3). These observations suggest that 1) infiltrating myeloid cells adopt microglia-like morphology in response to CNS milieu and 2) blood-derived cells persist in the CNS once lesions have been repaired. Co-immunolabeling with GFP and microglia/macrophage marker Iba1, T cell marker CD3, and B cell marker CD45R/B220 revealed that almost all GFP+ cells were of monocyte/macrophage origin (Fig. 3H-N), consistent with scarce lymphocytic infiltration in toxin-induced demyelinating lesions^{13, 14}. Numbers of Iba1+ cells were equal in GFP versus Sema3F mice, which shows that the overall inflammatory status was similar between these two groups. These numbers progressively decreased in time (Fig. 3O), as expected.

Thus, Sema3F-transduced cells generate macrophages in demyelinating CNS lesions.

Increased OPC repopulation and accelerated oligodendrogenesis and remyelination in Sema3F mice

Numbers of the PDGFR α + (OPCs) and Olig2+ (oligodendroglia) cells were quantified at 7 and 10 dpl, as OPC recruitment/proliferation is maximal within this time window (Fig. 4A), and were significantly higher in Sema3F mice at 7 dpl (Fig. 4B-D, E-G), while this increase was no longer significant at 10 dpl (Fig. 4D,G).

New oligodendrocytes in LPC lesions appear during second week post LPC (Fig. 4A). Numbers of APC/CC1+ cells (post-mitotic oligodendrocytes) were increased in Sema3F mice at both 7 and 10 dpl (Fig 4H-J), demonstrating accelerated generation of new oligodendrocytes.

We then quantified remyelination. Electron microscopy (EM) analyses of the lesions at the onset of remyelination (14 dpl) showed that, at this early time point, demyelinated axons were predominant in both groups. Interestingly, the proportion of axons surrounded by thin myelin sheaths was higher in Sema3F mice ($1.63 \pm 1\%$ in GFP versus $12.91 \pm 4.18\%$ in Sema3F mice), indicating a faster onset of remyelination (Fig. 4K-N).

Therefore, recruitment of Sema3F-expressing blood-derived macrophages to focal demyelinating lesions increases OPC repopulation, which accelerates oligodendrogenesis and myelin repair.

While it would have been interesting to confirm our results in a model of diffuse demyelination such as cuprizone intoxication, or in a model of autoimmune inflammation, the severity and high mortality risk in these models, incompatible with preconditioning protocols, precluded us from performing these experiments.

DISCUSSION

Enhancing remyelination using gene therapy?

While immunotherapies successfully halt the disease in a subset of patients with RRMS, scarce benefits are observed in progressive disease^{15, 16}, which suggests that reducing inflammation without regenerative/neuroprotective therapies at this stage does not prevent disability progression. Remyelination is associated with increased axonal survival in MS lesions². While several pro-remyelinating agents are current being tested, and certain phase 2 studies show interesting results (see⁵), the administration paradigm for these drugs is an unresolved issue. For example, oral administration may lead to extensive side effects and appears unsuitable for therapies that aim to stimulate local events in the lesion, such as OPC recruitment. Here we show that targeted molecular delivery to demyelinating lesions is possible using blood-derived macrophages as vehicles.

Peripheral macrophages are necessary for successful remyelination in mice^{17, 18}. Moreover, remyelination in old animals is accelerated by young blood-derived macrophages in parabiosis model^{18, 19}. This suggests that myelin repair can be improved simply by modifying monocytes recruited to the lesions. Our results suggest that genetic modification of monocytes/macrophages could be a clinically-relevant strategy to stimulate myelin repair. In addition to promoting OPC recruitment using Sema3F, this paradigm could also be used to overexpress neurotrophic factors and anti-oxidant molecules, which may be beneficial in progressive MS²⁰.

We have used transplantation of hematopoietic stem/progenitor cells as means of obtaining transgene-carrying monocytes/macrophages. Autologous hematopoietic stem cell transplantation (aHSCT) has been used to stabilize disease progression in RRMS, with little or no benefit observed in patients with progressive disease¹⁵. Theoretically, combining genetic modification of HSCs with autologous transplantation in clinic might potentially both regulate

inflammation and promote regeneration, thus extending the benefits of aHSC to a wider subset of patients. However, aHSC is associated with significant side effects and is therefore recommended only for a small subset of patients¹⁵. An alternative strategy, potentially applicable to a larger population of patients, may be to systemically deliver engineered monocytes amplified from autologous progenitor cells, as previously described²¹.

In conclusion, we provide a proof-of-concept that genetically-modified blood-derived macrophages increase OPC recruitment and accelerate CNS remyelination. These results combined with recent advances in gene therapy for human CNS diseases²² suggest our approach as a potentially useful therapeutic strategy to stimulate myelin repair and thus ultimately improve the long-term course of MS.

MATERIALS AND METHODS

A detailed version is provided in Supplemental Data.

Mice

Donors were 6-8-week old female and recipients 10-12 week-old male C57/Bl6 mice (Janvier, France). The experiments were performed according to the EU regulations and approved by the ethical committee for animal use (approval number 18471).

HSC culture and transduction

Mice were sacrificed, and bone marrow was flushed from tibias and femurs. Hematopoietic stem/progenitor cells were obtained by removing differentiated cells using Lin⁺ depletion kit. PGK-GFP (control) and PGK-GFP-T2A-Sema3F lentiviral vectors were applied at an MOI of 50.

Cells were maintained in culture for 5 days. GFP expression and viability were investigated using flow cytometry (Viability 405/520 Fixable Dye and propidium iodide). HSC proliferation/differentiation potential was assessed using colony-forming unit assay.

Western Blot

Proteins were extracted, size-separated by SDS-PAGE and transferred using Trans-Blot Turbo Midi Nitrocellulose Transfer Packs. Western blot for GFP and Sema3F was performed, and GADPH was used as a control.

OPC migration assay

Adult OPCs were isolated as described previously^{6, 10}. Migration in response to supernatant from non-transduced, PGK-GFP transduced-, or PGK-GFP-T2A-Sema3F-transduced HEK cells was assayed using transwell-chamber system (Corning, USA). At 24h, cells that have migrated were quantified. The assays were performed as duplicates or triplicates in 4 independent experiments. Log-normalized data were analyzed using two-way ANOVA.

Preconditioning and transplantation

Recipient mice were first pre-conditioned with cyclophosphamide (400mg/kg) and busulfan (100 mg/kg). This procedure enhances blood cell reconstitution by transplanted cells by inhibiting the proliferation of endogenous cells. Mice were then injected retro-orbitally with 600 000 HSCs.

Detection of chimerism

Eight weeks after transplantation, blood was extracted from transplanted mice. The proportion of donor cells was investigated by qPCR for sex determining region of the chromosome Y (SRY). Transduced (GFP+) cells were detected using flow cytometry.

Labeling for CD11b, CD3, and CD19 was performed to investigate the proportion of monocytes, T cells, and B cells, respectively, and analyzed using flow cytometry.

Demyelination

Demyelinating lesions were induced in the spinal cord, as described previously⁶.

Perfusion and tissue processing

Mice were perfused with a 4% paraformaldehyde (PFA; Sigma) solution in phosphate buffered saline (PBS) for immunohistochemical (IHC) analyses or 4% glutaraldehyde (Electron Microscopy Sciences) solution with CaCl_2 in phosphate buffer (PB) for electron microscopy (EM). Tissue was processed as described previously⁶.

Antibodies and immunohistochemistry

Detailed antibody information is provided in Supplemental data. Immunohistochemistry was performed as in⁶. Briefly, in all cases except for PDGFR α staining, antigen retrieval was performed by heating the sections in a low pH retrieval buffer (Vector Labs). Primary antibodies were applied overnight at 4°C. Secondary antibodies were applied for 1 hr, and nuclei were counterstained with DAPI.

Quantification

Images of demyelinating lesions (2-3 sections/mouse) were acquired using a TCS-STED-CW-SP8 super-resolution microscope (Leica) and imported into NIH ImageJ software. The area lacking myelin basic protein (MBP) staining was delimited, quantified, and cells positive for the marker(s) of interest within the lesion were counted.

For ultrathin sections, images of the lesion were taken using a transmission electron microscope (Hitachi) connected to a digital camera (AMT). Images were imported into ImageJ and remyelinated and demyelinated axons counted as described previously⁶.

Supplementary Material List

Materials and Methods (extended version)

Fig. S1. Scheme illustrating lentiviral vector constructions used in the study.

Fig. S2. Viability and proliferation/differentiation following Sema3F transduction in vitro.

Fig. S3. Morphology of GFP+ cells in the spinal cord.

Acknowledgements

We thank Dominique Langui and Asha Baskaran (BioImaging Core Facility-ICM Quant, Paris Brain Institute (ICM)), Catherine Blanc and Benedicte Hoareau (Flow Cytometry Core CyPS, Sorbonne Université, Pitié-Salpêtrière Hospital, Paris, France), and Laura Escobar and Juan Carlos Chara (Achucarro Basque Center for Neuroscience) for technical assistance; Alexis Bemelmans and Noelle Dufour (Molecular biology and vector production platform, MIRCEN, François Jacob Institute of Biology, CEA, Fontenay-aux-Roses, France) and Philippe Ravassard (ICM) for lentiviral vector production. We also thank Carlos Belmonte, Carlos Matute, Maria Domercq, and Sergio Lopez for their comments on the manuscript. This study was carried out at the cell culture (Celis) and preclinical functional exploration platform (PHENO ICMice) core facilities of the ICM (Paris, France), Achucarro Basque Center for Neuroscience Imaging Platform (Leioa, Spain), and “Analytical and High-resolution Microscopy in Biomedicine Platform” of the University of the Basque Country (Leioa, Spain).

Funding

This work was supported by the French National Institute of Health and Medical Research (INSERM), the French National Research Agency (ANR, project Stemimus ANR-12-BSV4-0002-02), the European Leukodystrophy Association (ELA, project ELA 2016-004C5B), NeurATRIS,

and the program “Investissements d'avenir” (ANR-10-IAIHU-06; (IHU-A-ICM)). VT was a recipient of the Spanish Ministry of Economy Young Investigator Grant (SAF2015-74332-JIN).

Author contributions

Conceived project VT, NC, and CL; Performed experiments: VT, GDC, MSA, BGL, ST, LI; Analyzed data: VT, MSA, GDC, BGL, ST, NC, CL.; Manuscript writing: VT, NC, and CL.

Conflict of interest

VT, GDC, MSA, BGL, ST, LI-nothing to disclose. NC- Scientific advisor for Asklepios Biopharmaceutics. Collaboration with Bluebird Bio; CL- participation to advisory boards for Roche, Biogen, Merck-Serono, Genzyme, Vertex, Rewind; scientific collaboration with Vertex and Merck Serono.

References

1. Lassmann, H., Pathogenic Mechanisms Associated With Different Clinical Courses of Multiple Sclerosis. *Front Immunol* **2018**, *9*, 3116.
2. Kornek, B.; Storch, M. K.; Weissert, R.; Wallstroem, E.; Stefferl, A.; Olsson, T.; Linington, C.; Schmidbauer, M.; Lassmann, H., Multiple sclerosis and chronic autoimmune encephalomyelitis: a comparative quantitative study of axonal injury in active, inactive, and remyelinated lesions. *Am J Pathol* **2000**, *157* (1), 267-76.
3. Irvine, K. A.; Blakemore, W. F., Remyelination protects axons from demyelination-associated axon degeneration. *Brain* **2008**, *131* (Pt 6), 1464-77.
4. Bodini, B.; Veronese, M.; García-Lorenzo, D.; Battaglini, M.; Poirion, E.; Chardain, A.; Freeman, L.; Louapre, C.; Tchikviladze, M.; Papeix, C.; Dollé, F.; Zalc, B.; Lubetzki, C.; Bottlaender, M.; Turkheimer, F.; Stankoff, B., Dynamic Imaging of Individual Remyelination Profiles in Multiple Sclerosis. *Ann Neurol* **2016**, *79* (5), 726-738.
5. Lubetzki, C.; Zalc, B.; Williams, A.; Stadelmann, C.; Stankoff, B., Remyelination in multiple sclerosis: from basic science to clinical translation. *Lancet Neurol* **2020**, *19* (8), 678-688.
6. Tepavčević, V.; Kerninon, C.; Aigrot, M. S.; Meppiel, E.; Mozafari, S.; Arnould-Laurent, R.; Ravassard, P.; Kennedy, T. E.; Nait-Oumesmar, B.; Lubetzki, C., Early netrin-1 expression impairs central nervous system remyelination. *Ann Neurol* **2014**, *76* (2), 252-68.

7. Moll, N. M.; Hong, E.; Fauveau, M.; Naruse, M.; Kerninon, C.; Tepavcevic, V.; Klopstein, A.; Seilhean, D.; Chew, L. J.; Gallo, V.; Nait Oumesmar, B., SOX17 is expressed in regenerating oligodendrocytes in experimental models of demyelination and in multiple sclerosis. *Glia* **2013**, *61* (10), 1659-72.
8. Boyd, A.; Zhang, H.; Williams, A., Insufficient OPC migration into demyelinated lesions is a cause of poor remyelination in MS and mouse models. *Acta Neuropathol* **2013**, *125* (6), 841-59.
9. Heß, K.; Starost, L.; Kieran, N. W.; Thomas, C.; Vincenten, M. C. J.; Antel, J.; Martino, G.; Huitinga, I.; Healy, L.; Kuhlmann, T., Lesion stage-dependent causes for impaired remyelination in MS. *Acta Neuropathol* **2020**, *140* (3), 359-375.
10. Piaton, G.; Aigrot, M. S.; Williams, A.; Moyon, S.; Tepavcevic, V.; Moutkine, I.; Gras, J.; Matho, K. S.; Schmitt, A.; Soellner, H.; Huber, A. B.; Ravassard, P.; Lubetzki, C., Class 3 semaphorins influence oligodendrocyte precursor recruitment and remyelination in adult central nervous system. *Brain* **2011**, *134* (Pt 4), 1156-67.
11. Williams, A.; Piaton, G.; Aigrot, M. S.; Belhadi, A.; Théaudin, M.; Petermann, F.; Thomas, J. L.; Zalc, B.; Lubetzki, C., Semaphorin 3A and 3F: key players in myelin repair in multiple sclerosis? *Brain* **2007**, *130* (Pt 10), 2554-65.
12. Prinz, M.; Priller, J.; Sisodia, S. S.; Ransohoff, R. M., Heterogeneity of CNS myeloid cells and their roles in neurodegeneration. *Nat Neurosci* **2011**, *14* (10), 1227-35.
13. Tepavcević, V.; Blakemore, W. F., Glial grafting for demyelinating disease. *Philos Trans R Soc Lond B Biol Sci* **2005**, *360* (1461), 1775-95.
14. Graça, D. L.; Blakemore, W. F., Delayed remyelination in rat spinal cord following ethidium bromide injection. *Neuropathol Appl Neurobiol* **1986**, *12* (6), 593-605.
15. Sharrack, B.; Saccardi, R.; Alexander, T.; Badoglio, M.; Burman, J.; Farge, D.; Greco, R.; Jessop, H.; Kazmi, M.; Kirgizov, K.; Labopin, M.; Mancardi, G.; Martin, R.; Moore, J.; Muraro, P. A.; Rovira, M.; Sormani, M. P.; Snowden, J. A.; (JACIE), E. S. f. B. a. M. T. E. A. D. W. P. A. a. t. J. A. C. o. t. I. S. f. C. T. I. a. E., Autologous haematopoietic stem cell transplantation and other cellular therapy in multiple sclerosis and immune-mediated neurological diseases: updated guidelines and recommendations from the EBMT Autoimmune Diseases Working Party (ADWP) and the Joint Accreditation Committee of EBMT and ISCT (JACIE). *Bone Marrow Transplant* **2020**, *55* (2), 283-306.
16. Lassmann, H., Targets of therapy in progressive MS. *Mult Scler* **2017**, *23* (12), 1593-1599.
17. Kotter, M. R.; Setzu, A.; Sim, F. J.; Van Rooijen, N.; Franklin, R. J., Macrophage depletion impairs oligodendrocyte remyelination following lysolecithin-induced demyelination. *Glia* **2001**, *35* (3), 204-12.
18. Ruckh, J. M.; Zhao, J. W.; Shadrach, J. L.; van Wijngaarden, P.; Rao, T. N.; Wagers, A. J.; Franklin, R. J., Rejuvenation of regeneration in the aging central nervous system. *Cell Stem Cell* **2012**, *10* (1), 96-103.
19. Miron, V. E.; Boyd, A.; Zhao, J. W.; Yuen, T. J.; Ruckh, J. M.; Shadrach, J. L.; van Wijngaarden, P.; Wagers, A. J.; Williams, A.; Franklin, R. J. M.; Ffrench-Constant, C., M2 microglia and macrophages drive oligodendrocyte differentiation during CNS remyelination. *Nat Neurosci* **2013**, *16* (9), 1211-1218.
20. Mahad, D. H.; Trapp, B. D.; Lassmann, H., Pathological mechanisms in progressive multiple sclerosis. *Lancet Neurol* **2015**, *14* (2), 183-93.
21. Li, B.; Baylink, D. J.; Walter, M. H.; Lau, K. H.; Meng, X.; Wang, J.; Cherkas, A.; Tang, X.; Qin, X., Targeted 25-hydroxyvitamin D3 1 α -hydroxylase adoptive gene therapy ameliorates dss-induced colitis without causing hypercalcemia in mice. *Mol Ther* **2015**, *23* (2), 339-51.
22. Piguet, F.; Alves, S.; Cartier, N., Clinical Gene Therapy for Neurodegenerative Diseases: Past, Present, and Future. *Hum Gene Ther* **2017**, *28* (11), 988-1003.

23. Kusy, S.; Funkelstein, L.; Bourgaïs, D.; Drabkin, H.; Rougon, G.; Roche, J.; Castellani, V., Redundant functions but temporal and regional regulation of two alternatively spliced isoforms of semaphorin 3F in the nervous system. *Mol Cell Neurosci* **2003**, *24* (2), 409-18.
24. Cresto, N.; Gaillard, M. C.; Gardier, C.; Gubinelli, F.; Diguët, E.; Bellet, D.; Legroux, L.; Mitja, J.; Auregan, G.; Guillermier, M.; Josephine, C.; Jan, C.; Dufour, N.; Joliot, A.; Hantraye, P.; Bonvento, G.; Déglon, N.; Bemelmans, A. P.; Cambon, K.; Liot, G.; Brouillet, E., The C-terminal domain of LRRK2 with the G2019S mutation is sufficient to produce neurodegeneration of dopaminergic neurons in vivo. *Neurobiol Dis* **2020**, *134*, 104614.

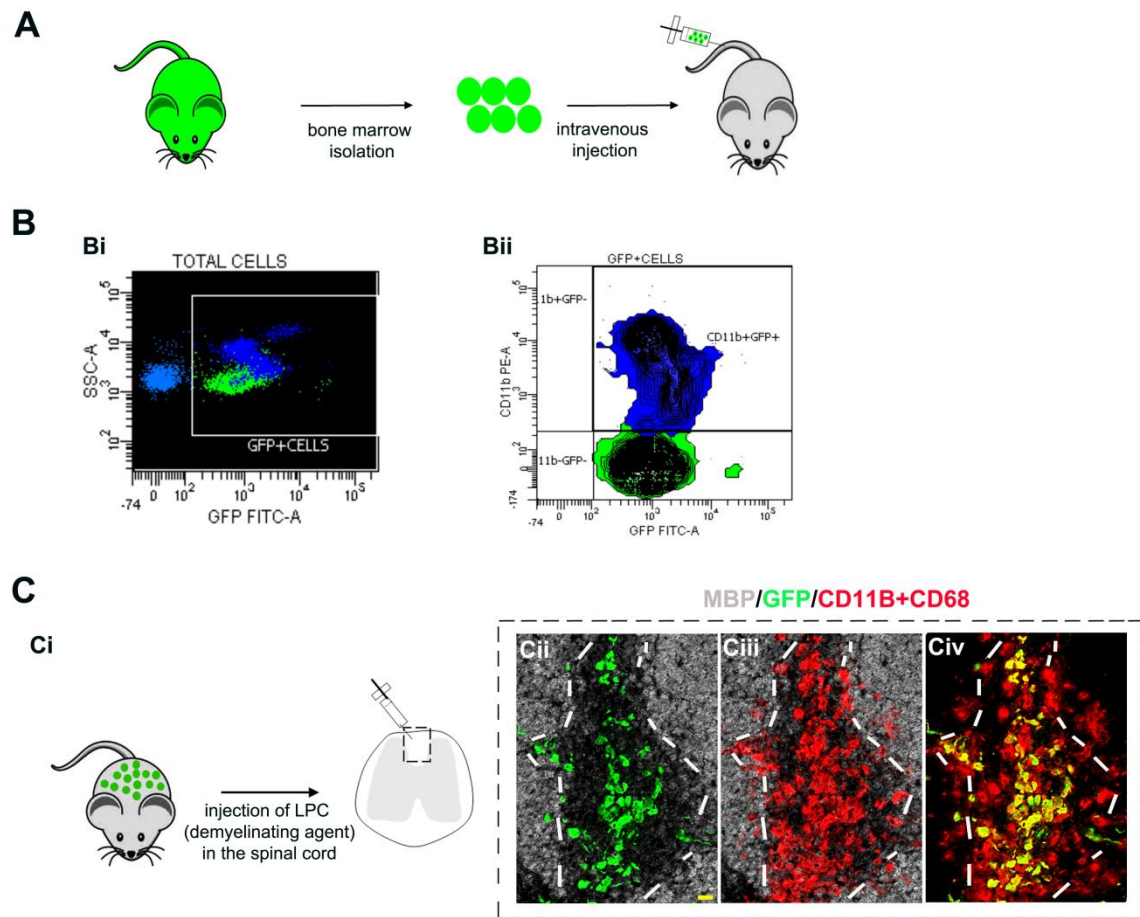


Figure 1. Graft- derived macrophages in demyelinating lesions **A.** Bone marrow was isolated from actin-GFP mice and transplanted into pre-conditioned recipient mice. **B.** Flow cytometry analyses of blood from recipient mice at 2 months post-transplant. **Bi.** Transplanted cells detected by GFP fluorescence. **Bii.** Labeling with CD11b shows that a large proportion of monocytes expresses GFP. **C.** Demyelinating lesions in chimeric mice at 3 dpl. **Ci.** Demyelination was induced in actin-gfp chimeras by injecting LPC, a demyelinating agent, in the spinal cord white matter. **Cii-Civ.** Co-immunolabeling for GFP, MBP, and a mixture of CD11b/CD68, showing graft-derived macrophages in the lesion. White lines indicate the borders of the lesion, identified by lack of MBP staining. Scale bar 20 μ m. MBP-myelin basic protein (gray); GFP-green fluorescent protein (green); CD11b/CD68-red.

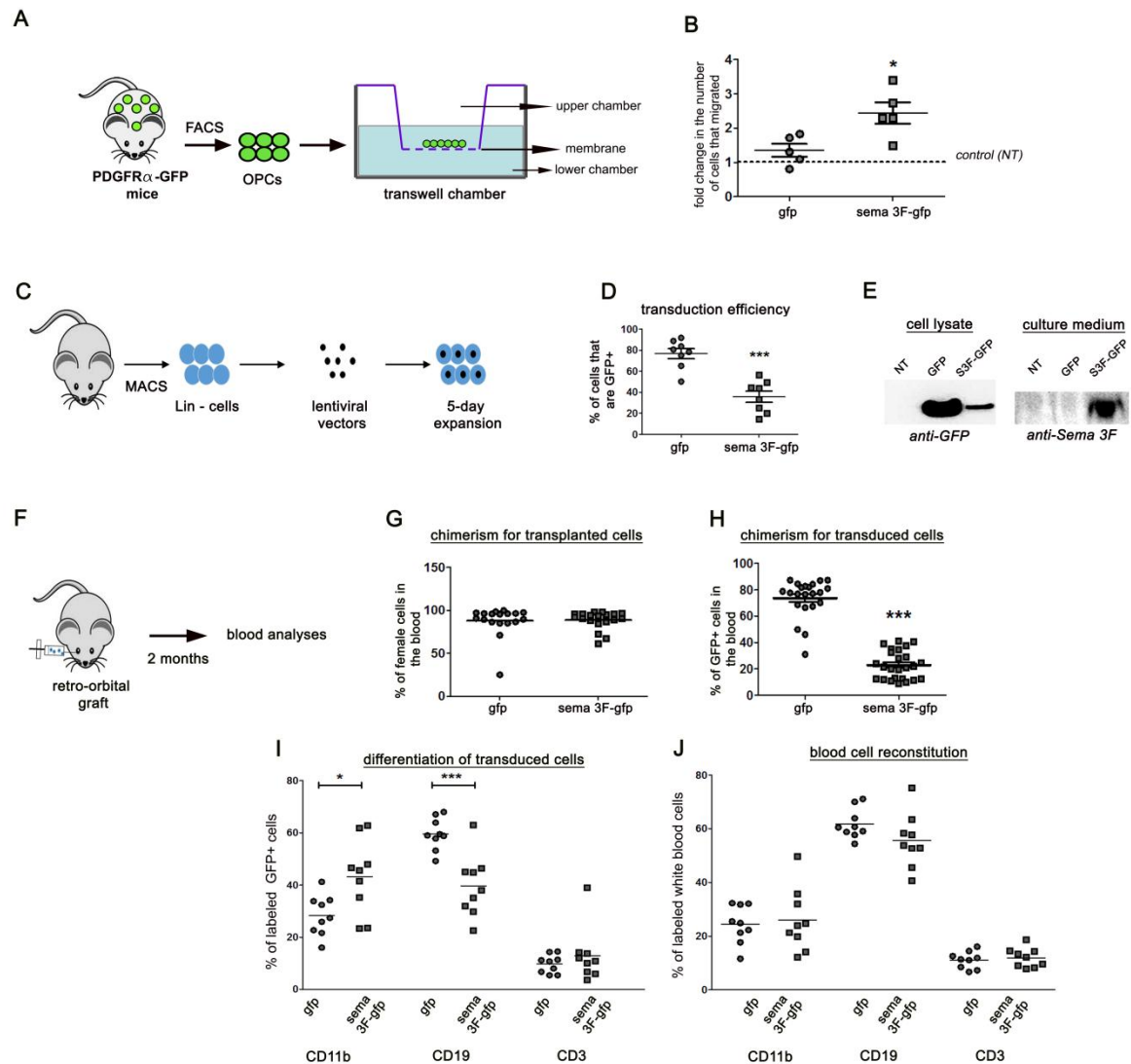


Figure 2. Generation of Sema3F chimeras. A-B. Transgene-encoded Sema3F increases OPC migration in vitro. A. OPCs isolated from adult PDGFR α -GFP mice using FACS were subjected to transwell-chamber migration assay with supernatants from non-transduced HEK cells (NT), GFP-transduced HEK, or Sema3F-transduced HEK added to the lower chamber. B. Results are presented as fold increase in cells that crossed the membrane insert with respect to the NT (dotted line). $p=0.01$. Student t test. $n=5$ independent experiments. C-E In vitro transduction of HSCs. C. Mouse bone marrow was isolated and differentiated cells (Lin⁺) were removed using MACS. Non-differentiated cells were transduced and expanded for 5 days. D. Numbers of GFP⁺ cells, verified using flow cytometry, are lower after transduction with Sema3F vector, $p<0.0001$, Student t test, $n=8$ independent experiments. E. Western blot. GFP expression in

cells transduced with GFP- and Sema3F -lentiviral vectors (at lower levels in the latter). Sema3F expression in the supernatant of Sema3F -transduced cells only. F-G. Transplantation and blood analyses. F. Transduced female HSCs were injected retro-orbitally into pre-conditioned male recipient mice. Blood was analyzed 2 months post-transplant. G. Percentage of transplanted (female) cells in the blood. n=18 -19 mice/group. H. Presence of transduced cells (GFP+) in the blood demonstrated using flow cytometry. $p<0.0001$. n=22-25 mice/group. I-J. Blood composition in GFP and Sema3F chimeras. I. Percentages of GFP+ cells labeled with CD11b, CD19, and CD3. The proportion of GFP+ cells labeled with CD11b is increased in Sema3F mice ($p=0.01$), that of cells labeled with CD19 is decreased ($p=0.0003$), and no differences are observed for CD3. J. Percentages of total blood cells positive for CD11b, CD19, and CD3 are the same among the groups. n=9 mice/group.

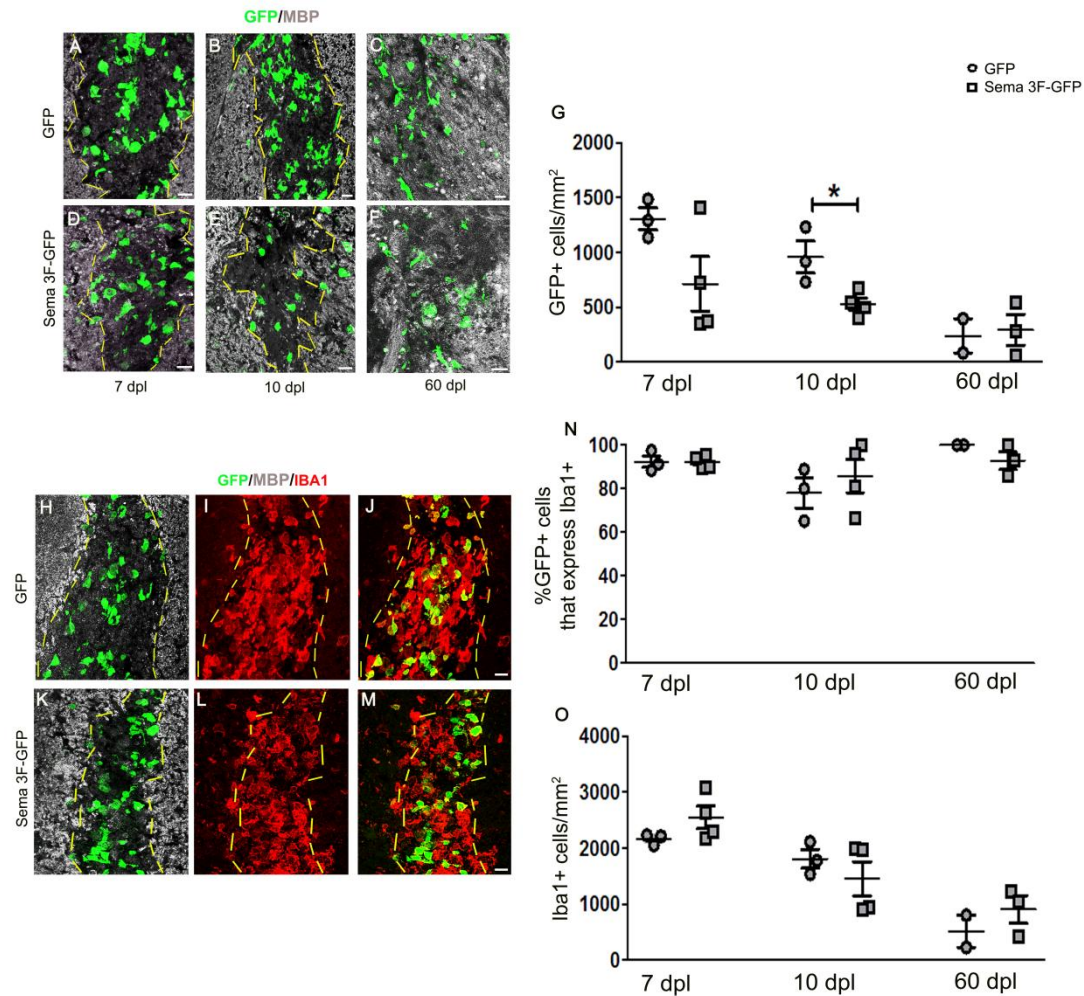


Figure 3. Transgene-carrying macrophages in demyelinating lesions. A-F. Co-labeling for GFP and MBP on spinal cord sections of GFP (A-C) and Sema3F-GFP chimeras (D-F) sacrificed at 7 (A,D), 10 (B,E), and 60 (C,F) dpl. Absence of MBP labeling in A-B,D-E indicates the area of demyelination at 7 and 10 dpl (delimited by yellow lines). Areas faintly labeled with MBP in C and F (60 dpl) likely represent areas that have undergone remyelination, but it is impossible to determine the extent of initial demyelination. **G.** Quantification of GFP+ cells ($p=0.02$). **H-M.** Co-labeling for GFP/MBP/Iba1 (macrophage/microglia marker). The absolute majority of GFP+ cells co-express Iba1. **N.** Percentages of GFP+ cells that are Iba1+ at 7, 10, and 60 dpl. **O.** Quantification of Iba1+ ($n=3-4$ mice /group for 7 and 10 dpl, $n=2-3$ mice/group for 60 dpl). Scale bars 20 μ m. Circles indicate GFP and squares Sema3F-GFP mice (G,N,O).

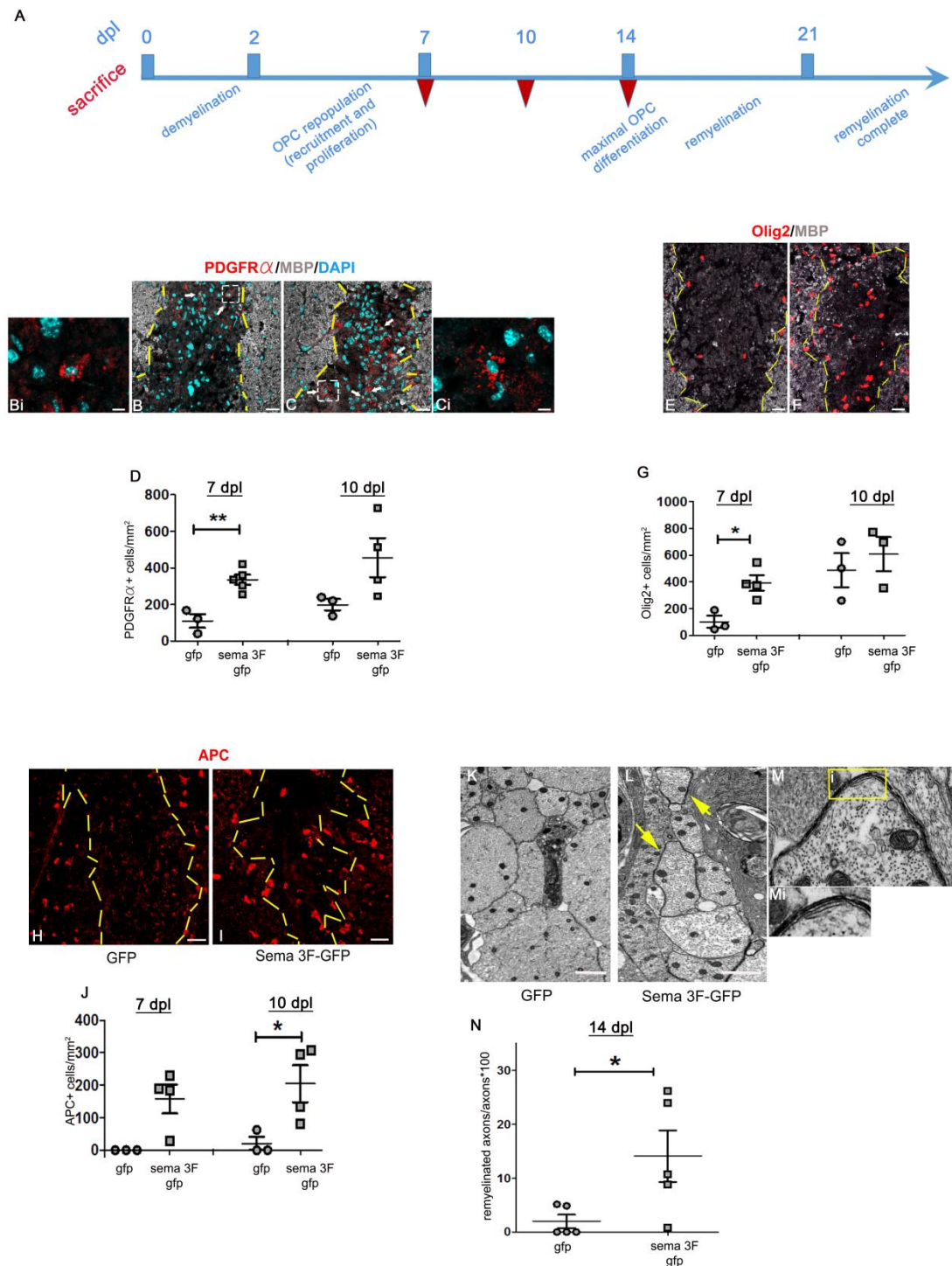


Figure 4. Increased OPC recruitment and accelerated oligodendrogenesis and remyelination in Sema3F chimeras. A. Temporal sequence of events in LPC model. dpl-days post lesion. Red inverted triangles indicate sacrifice. B-C, E-F. Lesions at 7 dpl in GFP (B,E) and Sema3F (C,F) mice. B-C. Co-labeling for PDGFR α (OPC marker), MBP, and DAPI. Arrows indicate OPCs in the

lesion. Bi and Ci-insets of white dotted squares in B and C. D. Higher numbers of PDGFR α + cells in Sema3F mice at 7 dpl ($p=0.0027$, $n=3-4$ mice/group). E-F. Co-labeling for oligodendroglial marker Olig2 and MBP. G. Higher numbers of Olig2+ cells in Sema3F-GFP mice at 7 dpl ($p=0.01$, $n=3-4$ mice/group). H-I. Labeling for APC/CC1, a marker of post-mitotic oligodendrocytes. Yellow dotted lines indicate the lesion border. APC+ cells in the normal tissue of GFP mice, but not in the lesion (H). I. APC+ cells in the lesion of Sema3F mice. J. Quantification of APC+ cells ($p=0.04$, $n=3-4$ mice/group). K-L. EM images of the lesion area in GFP (K) and Sema3F (L) chimeras at 14 dpl. While the axons in GFP mice remain demyelinated, a proportion of axons in Sema3F mice show thin myelin sheaths (yellow arrows). M. High power image of a newly generated myelin sheath in a Sema3F mouse. Mi. Magnified view of the area delimited by yellow square in M. N. Quantification of remyelinated axons ($p=0.04$, $n=5$ mice/group). Scale bars 20 μm (B,C,E,F,H,I), 5 μm (Bi, Ci), 1 μm (K,L).